Investigation of (Al$_2$O$_3$ & copper)/ water nanoparticles shape, slip effects and heat transfer on steady physiological delivery of MHD hybrid nanofluid.

Journal:	*Canadian Journal of Physics*
Manuscript ID	cjp-2018-0551.R1
Manuscript Type:	Article
Date Submitted by the Author:	05-Nov-2018
Complete List of Authors:	Iftikhar, Naheeda; University of Balochistan; Balochistan University of Information Technology and Management Sciences Rehman, Abdul; University of Balochistan, Quetta, Mathematics Sadaf, Hina; DBS&H, NUST, Islamabad Iqbal, Saleem ; University of Balochistan, Department of Mathematics
Keyword:	Peristaltic flow, Hybrid nanofluid, MHD, Shape effects, Exact solution
Is the invited manuscript for consideration in a Special Issue? :	Not applicable (regular submission)

SCHOLARONE™
Manuscripts

Study of (Al$_2$O$_3$ & copper)/ water nanoparticles shape, slip effects and heat transfer on steady physiological delivery of MHD hybrid nanofluid.

Naheeda Iftikhar[a,b] (Corresponding author)

[a]Department of Mathematics, University of Balochistan, Quetta, Pakistan

[b]Department of Mathematics, BUITEMS, Quetta, Pakistan

Email: naheeda_iftikhar@yahoo.com

[a*]Abdul Rehman: Department of Mathematics, University of Balochistan, Quetta, Pakistan

[b*]Hina Sadaf: DBS&H, CEME, National University of Sciences and Technology, Islamabad, Pakistan

[c*]Saleem Iqbal: Department of Mathematics, University of Balochistan, Quetta, Pakistan

Email: saleemiqbal81@yahoo.com

Abstract

The paper contains the analytical investigation of magnetohydrodynamic (MHD) flow of (Copper & Al$_2$O$_3$)/ water hybrid nanofluid with unstable peristaltic motion. Three different geometries (such as bricks, cylinder and platelets) along with velocity and thermal slip conditions are studied in detail in order to reach the precise solution. Flow geometry of a non-uniform tube of finite length, experimental values of base fluid and considered nanoparticles are taken into account to examine the theoretical investigation of formulated equations. Dimensionless control equations which are subject to physically realistic boundary conditions are closely studied to obtain precise results. The shape effects of nanoparticles on velocity, temperature distribution and heat transfer on the length of the non-uniform tube with variation of the various flow parameters are discussed in a graphical description to understand the theoretical aspects in order to validate the medical analysis. The observations from the analysis states that (Copper & Al$_2$O$_3$)/ water carry maximum velocity for smaller values of slip parameters. Temperature distribution for heat absorption parameter are more significant as fluid flow accelerates when large values are chosen. Large values of thermal slip parameter yield enhancement in pressure gradient and cu-water nanofluid

1

has higher impact than hybrid nanofluid. Platelets shape nanoparticles of hybrid nanofluid has more significant effect on pressure gradient as compare to cylinder and bricks shape nanoparticles of Cu-water nanofluid. An intrinsic property of peristaltic transport i.e trapping is also discussed. The trapped bolus decreases for platelets and cylinder shapes nanoparticles, whereas, the size of the trapped bolus increases for bricks shapes nanoparticles. This model is applicable to a drug delivery system and to design the micro peristaltic pump for transporting nanofluids.

Keywords: Peristaltic flow; Hybrid nanofluid; MHD; Shape effects; Exact solution

1. Introduction

The word "peristaltic movement" was derived from the Greek "peristaltikos" meaning clenching and compression. Peristaltic motion is a mechanism of fluid transport through deformable blood vessels with the aid of progressive contraction / expansion along the vessel. This is an important mechanism of fluid transport in different parts of physiological system.

Peristaltic flow also appears in the transport of urine from the kidneys to the bladder, sperm movement in the centrifuge of ducts of the male reproductive tract, vascular motion of small blood vessels such as arterioles, venues and capillaries. Peristaltic motion is practiced in industrial machines such as cardiopulmonary devices and roller pumps. Peristaltic apparatus was first clinically studied in articles written by Bayliss and Starling [1], however, Latham [2] theoretically examined the peristaltic movement using the principle of fluid dynamics. The study of Jaffrin and Shapiro [3] reveals various parameters of same process related to analysis of peristaltic pumps. Kumar et al. [4] studied transient peristaltic pumps in finite length tubes using permeable walls.

The interaction between peristaltic movement and heat transfer plays an important role in biomedicine. The same interaction has been analyzed to study the usage for hydrological, irrigation

2

and drainage problems as well as biological and environmental issues. The flow of nanofluids with heat transfer is a significant area of research for a variety of industrial and technical applications.

Recently, Conventional heat transfer fluids have been substituted by advanced liquids like nanofluorescence because it improves the heat transfer and flow characteristics of the fluid. The usage of nanoparticles in the heat exchanger not only reduces water flow but also reduces the volume and mass of the heat exchanger. Later, many examiners have erudite the functioning of heat exchangers by using nanofluid which showed definite improvement in the performance. In the beginning, Nanoparticles are used by Choi [5] which improved the thermal conductivity and rate of heat transfer in fluids. Nonetheless, few studies have been conducted on nanofluids in which various nanoparticles are dispersed at the same time in a base fluid commonly known as hybrid nanofluid. These nanofluids (hybrid) have many practical applications in real life. Ho a [6] have concluded that hybrid nanofluids, those work at very temperature, can effectively replace convective refrigerant. Hybrid nanofluids are the fluids that offer extremely better heat transfer and thermal properties than convective heat transfer fluids (oil, water and ethylene glycol) and nanofluids with single nanoparticles. This new nanotechnological fluid is synthesized by scattering two different nanoparticles in a conventional heat transfer fluid.

A substantial research is being conducted validating its use in electro and biosensors. Sphere/ carbon nanotube particles' applications on nanofluid was described by Han et al [7]. Stable nanofluid are formed when hybrid nanoparticles are dispersed to poly-alpha-olefin with a small amount of surfactants. An increase of 21% for particle volume fractions of 0.2% in effective thermal conductivity of fluids is observed in results.

Nine et al. [8] characterized the dispersion of CuO_2 and Cu - CuO_2 nanoparticles for the thermal enhancement. Thermal Performance of ZnO -TiO2 nanofluid is analyzed by Toghraie et al. [9]

3

which deals with temperature and concentration of nanoparticles. A recent review of hybrid nanofluid is being conducted by Sarkar et al. [10] who identifies hybrid nanofluids as perfect medium for effective heat transfer, however, many aspects in this filed are still unexplored and provide opportunity for researchers to dwell their research.

Almunia has low thermal conductivity of the metal nanoparticles but it does possess useful properties such as mass, chemical interness and stability. Aluminum, Copper, Silver and other metal nanoparticles possesses high thermal conductivity, however, the use of metal nanoparticles for nanofluid is limited because of strength and consistency of reactivity. The same properties of metallic, non-metallic nanoparticles and their compounds can improve stability and thermophysical property of nanofluids.

Han and Rhi [11] considered hybrid nanofluids and examined the thermal performance of channeled heat pipes. Selvakumar [12] examined heat transfer and pressure drop properties with Cu-Al_2O_3 / water hybrid nanofluid for electronic sinks and compared the hybrid Nanofluid (as cooling water) with deionized water and convective heat transfer. In addition, Suresh [13] studied an increase of 13.56% in Nusselt number of laminar flow convection using uniformly heated round tube, however, he observed maximum increase in Nusselt number. Nimmagada [14] examined the heat transfer properties of hybrid nanofluids $(Al_2O_3 + Ag)$ in the microchannel and ascertained coefficient of convective heat transfer. Allahyar et al. [15] investigated thermal performance of hybrid nanofluid at constant wall temperature in a curved heat exchanger and exhibited extreme heat transfer gain of 11.59%. Huang et al. [16] experimented heat transfer properties of hybrid nanofluid (Almunium oxide – Multiwall carbon nano tube) in Chevron Corrugated Sheet heat exchangers and introduced the highest coefficient of heat transfer for a given power pump. Takabi et al. [17] investigated hybrid aqueous suspension on the laminar convection effect of

4

Aluminaoxide and Copper nanoparticles. Devi [18] performed numerical studies of three-dimensional hybrid nanofluid (Cu- Al_2O_3 / water) flows on Lorentz force tensile sheets under Newtonian heating. Theoretically, limited studies on heat transfer with nanofluid and hybrid nanofluid phenomena are provided in literature like [19-34]. Few other studies [35-50] are also useful for this theoretical approach.

Magneto hydrodynamics (MHD) deals with the movement of highly conductive fluids through magnetic fields. Specifically, peristaltic motion in the existence of a magnetic field can be detected by conductivity such as geothermal source analysis, MHD generator design, hyperthermia therapy, drug delivery, elimination of arterial occlusion, MHD compressor, nuclear fuel debris treatment, underground control diffusion and contamination of chemical waste associated with processes related to material motion.

This work describes the hydrodynamic performance, thermal behavior of water-based hybrid suspension in a non-uniform tube for MHD flow. Analytical solutions were obtained for governing equations. Pertinent results for various parameters embedded in the system such as temperature, velocity, pressure gradient and pressure rise are discussed quantitatively and graphically. Further, this research work studies the comparison between the hydrodynamic and thermal behavior of the hybrid suspension by using a nanofluid having the same volume fraction for both nanoparticles and pure water. Theoretical importance and specialized utilization of this type of flow model makes it relevant in the field of mechanical engineering.

Nomenclatures

r^*, z^*	radial and axial direction in wave frame
d^*	wave speed
λ^*	wave length
k^*	non-uniform parameter
Φ^*	heat source/sink parameter
ε	Amplitude ratio
p^*	Pressure
Re	Reynolds's number
l_2^*	Radius of inner tube
L^*	velocity slip parameter
K^*_f	Thermal conductivity parameter
m^{**}	Different shape models
M^*	Hartmann number

2. Mathematical Formulation

The geometric model of the peristaltic flow phenomenon for two dimensional flow of an incompressible, electrically conducting viscous fluid with hybrid nanoparticles via in a non-uniform vertical tube (described in Fig.1 and Fig.2) is taken as

$R^*_2 = H^* = l^*(Z^*) + b^* \mathrm{Si}\,n\dfrac{2\pi}{\lambda^*}(Z^* - \mathrm{d}^*t^*)$. Whereas $l^*(Z^*) = l^*_2 * + k^* Z^*$ is the half width of

the inner tube at any axial distance Z^* from inlet and l_2 is the half width of the inlet, b^* is the

wave amplitude, λ^* is wavelength, Z^* axial coordinate, d^* shows the wave velocity, t^* is the

time and k^* is the non uniformity constant, when $k^* -> 0$, the non-uniform tube reduces to a

uniform tube.

The geometry of peristaltic motion is approached to a finite length of non-uniform tube whereas sinusoidal waves are travelling along the flow direction. Velocity slip, thermal slip and different shape effects are also employed. Flow equations are modelled by using cylindrical polar coordinate system $(r^*, 0, z^*)$ and reformed with low-Reynolds number rule and under supposition of long wavelength. z^*-axis is taken along the axis of the tube. The magnitude for temperature T^* at the wall of the tube $(R^* = R_2{}^*)$ are denoted as $T_1{}^*$, whereas, (Copper & Al_2O_3) nanoparticles and (water) base fluid have been considered in thermal stable environment. The mass, momentum and energy conservation equations along with nanoparticles and MHD can be termed as:
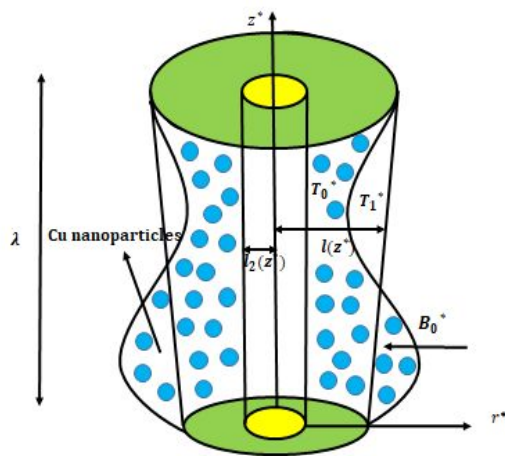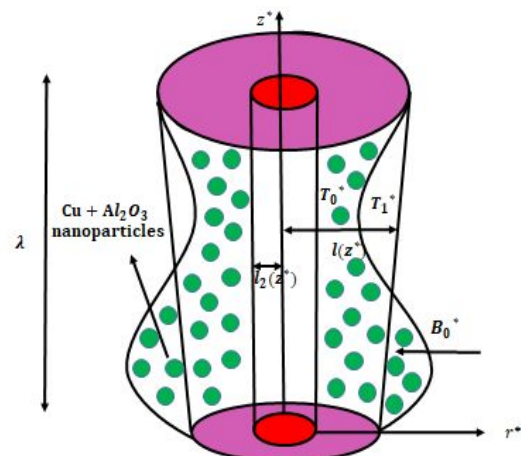
Fig. 1   **Fig. 2**

Flow Geometry

It is not an easy preposition to reach an equation that is universal for both compressible and incompressible flow regimes, hence, precise solution for both equations cannot be obtained in totality. This is because of the difference in mathematical characters of governing equations, hence, problems regarding fluid mechanism are solved for one of these equations.

7

Continuity Equation

$$\frac{\partial}{\partial} + \nabla.\left(\vec{V}\right) = 0,$$ (1)

For incompressible flow Eq. (1) reduces to $\nabla.\vec{V} = 0$

$$\nabla.\vec{V} = \frac{1}{R^*}\frac{\partial}{\partial R^*}(R^* U^*) + \frac{1}{R^*}\frac{\partial V^*}{\partial \theta^*} + \frac{\partial W^*}{\partial Z^*}$$ (2)

By using our assumptions $(r^*, 0, z^*)$ Eq. (2) becomes

$$\nabla.\vec{V} = \frac{1}{R^*}\frac{\partial}{\partial R^*}(R^* U^*) + \frac{\partial W^*}{\partial Z^*}$$

$$\frac{\partial U^*}{\partial R^*} + \frac{\partial W^*}{\partial Z^*} + \frac{U^*}{R^*} = 0$$ (3)

Momentum Equation

Linear momentum conservation equations can also be termed as Navier-Stokes equation. There are many other forms to write the same equation. It is possible to write it in many different forms. The reduction in viscous stress tensor for incompressible flows cane be expressed as: -

$$\rho^*{}_{hnf}\left[\frac{\partial \vec{V}}{\partial} + \left(\vec{V}.\nabla\right)\vec{V}\right] = -\nabla P^* + \nabla.\tau_{R^* Z^*} + \rho^*{}_{hnf}$$ (4)

$$\rho^*{}_{hnf}\left[\frac{\partial \vec{V}}{\partial} + \left(\vec{V}.\nabla\right)\vec{V}\right] = -\nabla P^* + \mu\nabla^2\vec{V} + \rho^*{}_{hnf}$$ (5)

Momentum Eq. in cylindrical coordinate system after the contribution of magnetic field in axial direction are: -

$$\rho^*{}_{hnf}\left[\frac{\partial U^*}{\partial t^*} + U^*\frac{\partial U^*}{\partial R^*} + W^*\frac{\partial U^*}{\partial Z^*}\right] = -\frac{\partial P^*}{\partial R^*} + \mu^*{}_{hnf}\left[\frac{1}{R^*}\frac{\partial}{\partial R^*}\left(R^*\frac{\partial U^*}{\partial R^*}\right) + \frac{\partial^2 U^*}{\partial Z^{*2}} - \frac{U^*}{R^{*2}}\right]$$ (6)

$$\rho^*{}_{hnf}\left[\frac{\partial U^*}{\partial t^*} + U^*\frac{\partial W^*}{\partial R^*} + W^*\frac{\partial W^*}{\partial Z^*}\right] = -\frac{\partial P^*}{\partial Z^*} + \mu^*{}_{hnf}\left[\frac{1}{R^*}\frac{\partial}{\partial R^*}\left(R^*\frac{\partial W^*}{\partial R^*}\right) + \frac{\partial^2 W^*}{\partial Z^{*2}}\right] +$$

$$(\rho\beta)^{*}_{hnf}\, g^{*}(T^{*}-T_{1})-\frac{\sigma^{*}_{hnf}}{\sigma^{*}_{f}}\frac{B^{*}_{o}{}^{2}}{R^{*2}}\, W^{*} \tag{7}$$

Energy Equation

Energy Eq. can be expressed as: -

$$\rho^{*}_{hnf}\left[\frac{\partial h}{\partial t^{*}}+\nabla.(h\vec{V})\right]=-\frac{DP^{*}}{Dt^{*}}+\nabla.(k^{*}\nabla T^{*})+\emptyset$$

(8)

h is the enthalpy which is in connection with specific internal energy. T^{*} represents absolute

temperature and $\emptyset$ shows constant heat absorption parameter.

Pressure term on R.H.S of Eq. (8) is commonly ignored. In order to find energy equation the

conduction heat transfer is directed by Fourier's law with existence of k^{*}_{hnf} (thermal conductivity)

of the hybrid nanofluid. Also note that radiative heat transfers and internal heat generation due to

a possible chemical or nuclear reaction are neglected. For an ideal gas it is possible to use the

following relations to relate enthalpy and internal energy to temperature so that energy equation

can be written as temperature being the only unknown.

$$dh = c_{p}{}^{*}\, dT^{*}$$

(9)

By taking into account the fact that for incompressible flows, density is constant. By using the

relation in Eq. (9), the energy equation takes the following form

$$(\rho^{*}c_{p}{}^{*})_{hnf}=\left[\frac{\partial T^{*}}{\partial t^{*}}+(\vec{V}.\nabla)T^{*}\right]=k^{*}_{hnf}\,\nabla^{2}T^{*}+\emptyset$$

(10)

The energy equation is

$$(\rho^{*}c_{p}{}^{*})_{hnf}\left[\frac{\partial T^{*}}{\partial t^{*}}+U^{*}\frac{\partial T^{*}}{\partial R^{*}}+W^{*}\frac{\partial T^{*}}{\partial Z^{*}}\right]=k^{*}_{hnf}\left[\frac{\partial^{2}T^{*}}{\partial R^{*2}}+\frac{1}{R^{*}}\frac{\partial T^{*}}{\partial R^{*}}+\frac{\partial^{2}T^{*}}{\partial Z^{*2}}\right]+Q^{*}_{0} \tag{11}$$

9

In all above equations, σ^*_{hnf} shows the density of hybrid nanofluid, U^* and W^* are the relatively velocity components in radial and axial directions, $(\rho c_p)^*_{hnf}$ represents heat capacity of hybrid nanofluid, μ^*_{hnf} is viscosity of hybrid nanofluid and k^*_{hnf} represents thermal conductivity of hybrid nanofluid, P^* is pressure, g^* is the acceleration due to gravity, Q^*_0 constant heat absorption parameter and β^*_{hnf} is the thermal expansion coefficient of hybrid nanofluid.

Initially we have added the solid volume fraction of Cu (φ_1) to the base fluid with 0.1 vol (i.e., φ_1 =0 .1 i.e. fixed hereafter) nanoparticle and subsequentially Al_2O_3 (φ_2) is added with variation of volume fractions $(0.005 \leq \varphi_2 \leq 0.06)$ for the formation of (Cu− Al_2O_3/Water) hybrid nanofluid. Whereas, thermophysical properties for water intervening hybrid nanofluid are demarcated as follows [51]: -

Properties	Nanofluid
Thermal Diffusivity	$\alpha^*_{nf} = \dfrac{k^*_{nf}}{(\rho c_p)^*_{nf}}$,
Viscosity	$\mu^*_{nf} = \dfrac{\mu^*_f}{(1-\varphi)^{2.5}}$,
Electrical conductivity	$\sigma^*_{nf} = \sigma^*_{bf}\left[\dfrac{\sigma_s(1+2\varphi)+2\sigma^*_{bf}(1-\varphi)}{\sigma_s(1-\varphi)+\sigma^*_{bf}(2+\varphi)}\right]$,
Thermal conductivity (12)	$\dfrac{k^*_{nf}}{k^*_f} = \dfrac{k^*_s+(m-1)k^*_{bf}-(m-1)(k^*_{bf}-k^*_s)\varphi}{k^*_s+(m-1)k^*_{bf}+(k^*_{bf}-k^*_s)\varphi}$,
Density	$\rho^*_{nf} = \rho^*_f(1-\varphi)+\varphi\left(\rho^*_s \big/ \rho^*_f\right)$,
Heat capacity	$(\rho c_p)^*_{nf} = (1-\varphi)\left[(1-\varphi)(\rho c_p)^*_f + \varphi(\rho c_p)^*_s\right]$,
Thermal expansion	$(\rho\beta)^*_{nf} = (\rho\beta)^*_f\left[(1-\varphi)+\varphi\left((\rho\beta)^*_s \big/ (\rho\beta)^*_f\right)\right]$

10

Properties	Hybrid Nanofluid

Thermal Diffusivity

$$\alpha^*{}_{hnf} = \frac{k^*{}_{hnf}}{(\rho c_p)^*{}_{hnf}},$$

Viscosity

$$\mu^*{}_{hnf} = \frac{\mu^*{}_f}{(1-\varphi_2)^{2.5}(1-\varphi_1)^{2.5}},$$

Electrical conductivity

$$\sigma^*{}_{hnf} = \sigma^*{}_{bf}\left[\frac{\sigma_{s2}(1+2\varphi_2)+2\sigma^*{}_{bf}(1-\varphi_2)}{\sigma_{s2}(1-\varphi_2)+\sigma^*{}_{bf}(2+\varphi_2)}\right],$$

where $\sigma^*{}_{bf} = \sigma^*{}_f\left[\frac{\sigma_{s1}(1+2\varphi_1)+2\sigma^*{}_f(1-\varphi_1)}{\sigma_{s1}(1-\varphi_1)+\sigma^*{}_f(2+\varphi_1)}\right],$

Thermal conductivity

$$\frac{k^*{}_{hnf}}{k^*{}_{bf}} = \frac{k^*{}_{s2}+(m-1)k^*{}_{bf}-(m-1)(k^*{}_{bf}-k^*{}_{s2})\varphi_2}{k^*{}_{s2}+(m-1)k^*{}_{bf}+(k^*{}_{bf}-k^*{}_{s2})\varphi_2},$$

Where $\frac{k^*{}_{bf}}{k^*{}_f} = \frac{k^*{}_{s1}+(m-1)k_f{}^*-(m-1)(k_f-k^*{}_{s1})\varphi_1}{k^*{}_{s1}+(m-1)k_f{}^*+(k_f{}^*-k^*{}_{s1})\varphi_1},$

Density

$$\rho^*{}_{hnf} = \rho^*{}_f(1-\varphi_1)(1-\varphi_2)+\varphi_1\left(\rho^*{}_{s1}\big/\rho^*{}_f\right)+\varphi_2\rho^*{}_{s2},$$

Heat capacity

$$(\rho c_p)^*{}_{hnf} = (1-\varphi_2)\left[(1-\varphi_1)(\rho c_p)^*{}_f+\varphi_1(\rho c_p)^*{}_{s1}\right]+\varphi_2(\rho c_p)^*{}_{s2},$$

Thermal expansion

$$(\rho\beta)^*{}_{hnf} = (\rho\beta)^*{}_f(1-\varphi_2)\left[(1-\varphi_1)+\varphi_1\left((\rho\beta)^*{}_{s1}\big/(\rho\beta)^*{}_f\right)\right]+\varphi_2(\rho\beta)^*{}_{s2},$$

Where φ_1 and φ_2 are the correspondence of solid volume fraction of Al_2O_3 and Cu nanoparticles. Whereas $s1$ denotes solid nanoparticles of copper, $s2$ solid nanoparticles of Alumina, f represents $fluid$, nf, hnf shows nano and hybrid nanofluid respectively. $\varphi_1, \varphi_2 = 0$ corresponds to the pure water (without suspension of nanoparticles).

Nanoparticles Category	Shape Factor (m'')	Shape
Bricks	3.7	
Cylinders	4.9	

	5.7	
Platelets		
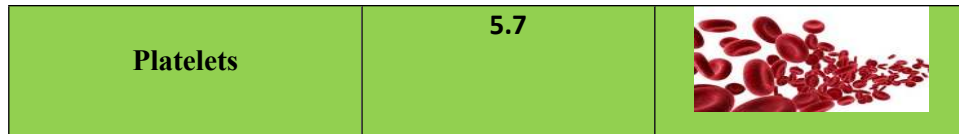
According to the geometry, the pertinent boundary conditions for the raised problem (shown in Fig. 1, Fig. 2) are defined as: -

$$W^* = 0, \qquad at \quad R^* = R_1^*,$$

$$W^* - W_w^* = -L^* \, \tau_{R^*Z^*}, \quad at \ R_2^* = H^* = l^*(Z^*) + b^* \, \mathrm{Si} \, n \frac{2\pi}{\lambda^*}(Z^* - d^*t^*),$$

$$T^* = T_0^*, \quad at \quad R^* = R_1^*,$$

$$T^* - T_1^* = -\gamma^* \frac{\partial T^*}{\partial R^*}, \ at \ R^* = R_2^*,$$

(13)

Where W^* is the fluid velocity, whereas H^* symbolizes the non-uniform wave in which $l^*(Z^*)$ is the non-uniform radius, l^* (radius of inner tube), b^* (wave amplitude) and γ^* (thermal slip) and L^* (velocity slip) are the dimensional parameters.

Non-dimensional parameters are given below to linearize the problem:

$$r^* = \frac{R^*}{l_2^*}, \ z^* = \frac{Z^*}{\lambda^*}, \ u^* = \frac{\lambda^* U^*}{l_2^* d^*}, \ w^* = \frac{W^*}{d^*}, \ P^* = \frac{l_2^{*2} p^*}{\lambda^* \mu_f^* d^*}, \ t^* = \frac{d^* t''}{\lambda^*}, \ L = \frac{\mu_f^* L^*}{l_2^*}, \ \gamma = \frac{\gamma^*}{l_2^*},$$

$$\mathrm{Re} = \frac{\rho_f^* d^* l_2^*}{\mu_f^*}, \ \theta^* = \frac{T^* - T_1^*}{T_0^* - T_1^*}, \ l^*(Z^*) = l_2^* + k^* z^*, \ h^* = \frac{H^*}{l_2^*} = 1 + \frac{\lambda^* k^* z^*}{l_2^*} + \varepsilon \sin 2\pi(z^* - t^*), \ (14)$$

$$\tau = \frac{l_2^* \tau^*}{d^* \mu_0^*}, \ K'' = \frac{K}{l_2^*}, \ B^* = \frac{Q_0^* l_2^{*2}}{(T_0^* - T_1^*)k_f^*}, \ G_r = \frac{(T_0^* - T_1^*)g^* \beta_f^* \rho_f^* l_2^{*2}}{d^* \mu_f^*}, \ M^{*2} = \frac{\rho_f^*}{\mu_f^*} B_o^{*2} d^*.$$

B^*, L, γ denote heat absorption, velocity and thermal slip parameter. By arranging Eq. (14) into Eqs. (3), (6), (7) and (11) and taking the conditions of long wavelength approach (peristaltic wavelength is much larger then tube) qualifies that $\delta \rightarrow 0$ and Reynolds number is relative to viscous damping forces. By omitting the terms containing $R_e \rightarrow 0$, δ and higher we have the next equations, numbers also vanishes. $\delta \rightarrow 0$ reflects curvature effects and $R_e \rightarrow 0$ contradicts convective inertial forces. Implementation of these approximations to Eq. (3), (6), (7), (11) and (13) results:-

$$\frac{\partial p^*}{\partial r^*} = 0, \tag{15}$$

$$-\frac{\partial p^*}{\partial z^*} + \frac{\mu^*_{hnf}}{\mu^*_f}\left[\frac{1}{r^*}\frac{\partial}{\partial r^*}(r^*\frac{\partial w^*}{\partial r^*})\right] + \frac{(\rho\beta)^*_{hnf}}{(\rho\beta)^*_f}G_r\theta^* - \frac{\sigma^*_{hnf}}{\sigma^*_f}\frac{M^{*2}}{r^{*2}}w^* = 0 \tag{16}$$

$$\frac{\alpha^*_{hnf}}{\alpha^*_f}\left[\frac{1}{r^*}\frac{\partial\theta^*}{\partial r^*} + \frac{\partial^2\theta^*}{\partial r^{*2}}\right] + B^*\frac{(\rho c_p)^*_f}{(\rho c_p)^*_{hnf}} = 0, \tag{17}$$

Where $\alpha^*_{hnf} = \dfrac{k^*_{hnf}}{(\rho c_p)^*_{hnf}}$, by using in Eq. (17) we get the following form

$$\frac{k^*_{hnf}}{(\rho c_p)^*_{hnf}\alpha^*_f}\left[\frac{1}{r^*}\frac{\partial\theta^*}{\partial r^*} + \frac{\partial^2\theta^*}{\partial r^{*2}}\right] + B^*\frac{(\rho c_p)^*_f}{(\rho c_p)^*_{hnf}} = 0, \tag{18}$$

$$\frac{k^*_{hnf}}{\alpha^*_f}\left[\frac{1}{r^*}\frac{\partial\theta^*}{\partial r^*} + \frac{\partial^2\theta^*}{\partial r^{*2}}\right] + B^*(\rho c_p)^*_f = 0, \tag{19}$$

By considering $A = \dfrac{\mu^*_{hnf}}{\mu^*_f}, T = \dfrac{(\rho\beta)^*_{hnf}}{(\rho\beta)^*_f}, F = \dfrac{\sigma^*_{hnf}}{\sigma^*_f}, S = (\rho c_p)^*_f$ and $H = \dfrac{k^*_{hnf}}{\alpha^*_f}$. Using in Eq. (16) and (19), we get

$$\frac{\partial p^*}{\partial r^*} = 0, \tag{20}$$

$$-\frac{\partial p^*}{\partial z^*} + A\left[\frac{1}{r^*}\frac{\partial}{\partial r^*}(r^*\frac{\partial w^*}{\partial r^*})\right] + TG_r\theta^* - F\frac{M^{*2}}{r^{*2}}w^* = 0 \tag{21}$$

$$H\left[\frac{1}{r^*}\frac{\partial\theta^*}{\partial r^*} + \frac{\partial^2\theta^*}{\partial r^{*2}}\right] + B^*S = 0, \tag{22}$$

With boundary conditions

$\theta^* = 1 \quad at \quad r^* = r_1^*$

$\theta^* + \gamma\dfrac{\partial\theta^*}{\partial r^*} = 0 \ at \ r^* = r_2^*$

(23)

$w^* = -1 \ at \ r^* = r_1^*$

$w^* + LA\dfrac{\partial w^*}{\partial r^*} = 0 \ at \ r^* = r_2^*$

(24)

Numerical values are apropos in **Table 1**.

13

Physical properties	Fluid Phase	Solid Nanoparticles	
	Water	Copper	Al$_2$O$_3$
$c^*_p\left(\frac{J}{kgK}\right)$	4179	385	765
$\rho^*\left(\frac{kg}{m^3}\right)$	997.1	8933	3970
$K^*_f\left(\frac{W}{m.k}\right)$	0.613	401	40
$\sigma\left(\frac{S}{m}\right)$	5.5×10^{-6}	59.6×10^6	35×10^6

Table 1. Thermophysical properties of fluid and nanoparticles.[47]

3. Solution to the problem

Exact solution of Eq. (21) and (22) by using boundary conditions of (23) and (24) can be determined by Cauchy Euler's method.

$$\theta^* = -\frac{BS(r^*)^2}{4H} + C_1 Log(r^*) + C_2$$

$$(25) \quad w^* = C_3(r^*)^{-M^*\sqrt{F/A}} + C_4\,(r^*)^{M^*\sqrt{F/A}} - \frac{\partial P/\partial Z}{A}\left(\frac{(r^*)^2}{4-(M^*)^2\frac{F}{A}}\right) - \frac{T*G}{A}$$

$$\left(\frac{(r^*)^2}{4-(M^*)^2\frac{F}{A}} + \frac{BS}{4H}\left(\frac{(r_1^*)^2(r^*)^2}{4-(M^*)^2\frac{F}{A}} - \frac{(r^*)^4}{16-(M^*)^2\frac{F}{A}}\right) + \frac{BS(r_1^*r_2^*)}{4H}\left(\frac{(r_2^*)^2-(r_1^*)^2}{\gamma r_1^*+r_2^*Log(r_2^*)}\left(\frac{(r^*)^2Log(r^*)}{4-(M^*)^2\frac{F}{A}} - \frac{2(r^*)^2}{(4-(M^*)^2\frac{F}{A})^2}\right) + \frac{2\gamma r_2^*}{\gamma r_1^*+r_2^*Log(r_2}\right.$$

(26)

Where $C_1, C_2, C_3\ and\ C_4$ are constants calculated by Mathematica.

The pressure rise ΔP^* is defined as follows

$$\Delta P^* = \int_0^1 -\frac{dP^*}{dz^*}\,dz^*, \qquad (27)$$

Velocities in expressions of stream function relation can be defined as

$$u^* = -\frac{1}{r^*}\frac{\partial \Psi}{\partial z^*}, \ w^* = \frac{1}{r^*}\frac{\partial \Psi}{\partial z^*} \quad at \quad r^* = h^*$$

And heat transfer on walls are expressed as

$$Z_2 = \left(\frac{\partial \theta^*}{\partial r^*}\right)\left(\frac{\partial h^*}{\partial z^*}\right) \ at\ r^* = r_2^* \qquad (28)$$

14

z^*	Z_2 for B=1.0 Cu/Water	Z_2 for B=1.0 (Copper & Al$_2$O$_3$)/ water	Z_2 for B=1.5 Cu/Water	Z_2 for B=1.5 (Copper & Al$_2$O$_3$)/ water	Z_2 for B=2.0 Cu/Water	Z_2 for B=2.0 (Copper & Al$_2$O$_3$)/ water
-1.02	0.779768	0.779896	0.779487	0.779679	0.779487	0.779463
-0.82	0.745714	0.747253	0.742339	0.744648	0.742339	0.742042
-0.62	0.782827	0.783864	0.780552	0.782108	0.780552	0.780351
-0.42	0.826092	0.823717	0.831299	0.827737	0.831299	0.831758
-0.22	0.830347	0.826813	0.838098	0.832796	0.838098	0.83878
-0.02	0.793439	0.794346	0.791449	0.79281	0.791449	0.791274
0.18	0.763772	0.769455	0.75131	0.759834	0.75131	0.750213
0.38	0.783522	0.786341	0.777339	0.781568	0.777339	0.776795
0.58	0.829983	0.824551	0.841897	0.833748	0.841897	0.842946
0.78	0.838244	0.83103	0.854064	0.843243	0.854064	0.855456
0.98	0.791287	0.792985	0.787566	0.790111	0.787566	0.787238

Table 2. Heat transfer result for both fluids.

4. Results evaluation and discussion

In order to comprehend this problem, the eminent features of the velocity, temperature, pressure rise, pressure gradient and stream lines pattern of the fluid are obtained using (Cu-water) nanofluid and hybrid (Cu-Al$_2$O$_3$/ water) nanofluid in a non-uniform tube. Initially, the nanoparticle of Cu (φ_1) is added to the base fluid and subsequently Al$_2$O$_3$ (φ_2) is added. Parametric study has been made for the graphical results which shows precise solutions and are shown as under: -

Figs. (3-6) depict the trend of velocity distribution for solid volume fraction of (Cu- Al$_2$O$_3$)/water and Cu/Water. Substantially, the nanoparticles dissipate energy in the form of heat. At once the velocity for both nanofluid and hybrid nanofluid is improved with addition of more nanoparticles. Fig.3 portray the effects of slip parameter on hybrid nanofluid and nanofluid. It shows that velocity has decreasing behavior for large values of velocity slip parameter. Same effect of thermal slip parameter on velocity profile is witnessed in Fig. 4. The results reveals that Cu-water/nanofluid is

15

slower than the hybrid nanofluid for large values of slip parameters. Figs. (3-4) shows that velocity

of the hybrid/nanofluid is always higher than the Cu-water nanofluid whatever the values of the

slip parameters are taken. It also describes that slip shows reduction in the velocity field. The same

slip retards the fluid motion which ultimately exhibits a decrease in the fluid nanoparticles. Impacts

of different shape of nanoparticles are plotted in Figs. (3-6) It is concluded from Fig. 5 that velocity

decelerates when heat absorption parameter increases. Fig. 6. It is evidently accentuated that

nanoparticles velocity has maximum increase with the shape of platelets. Figs. (3-6) illustrates that

velocity is elevated while using hybrid nanofluid as compared to cu/water nanofluid.
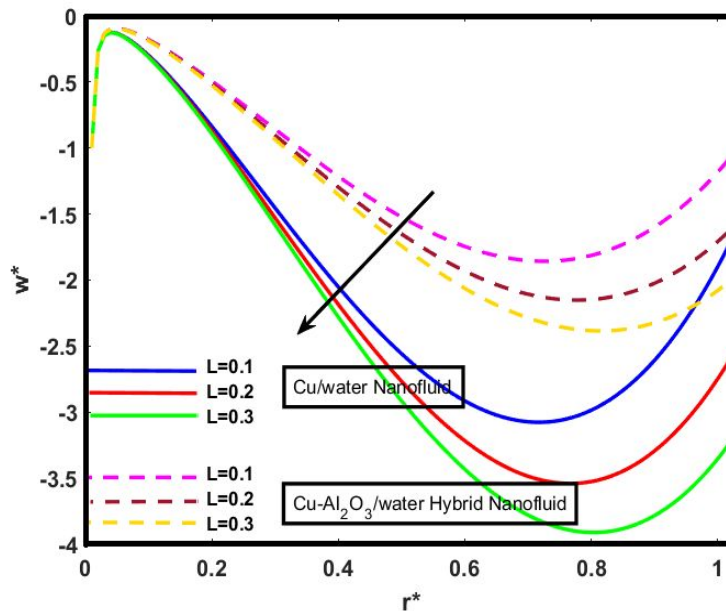
Fig. 3: Velocity distribution for different values of L and $z^* = 0.2$, $L=0.1$, $\lambda=0.1$, $\gamma=0.1$, G_r^* =0.2, M=2, $Q = 0.01$, $t^{**} = 0.2$, $k^* = 0.3$, $m' = 3.7$, $B = 1.0$,

$$\varphi_1 = 0.1, \varphi_2 = 0.02 \ (Cu - Al_2O_3/water \ Nanofluid),$$

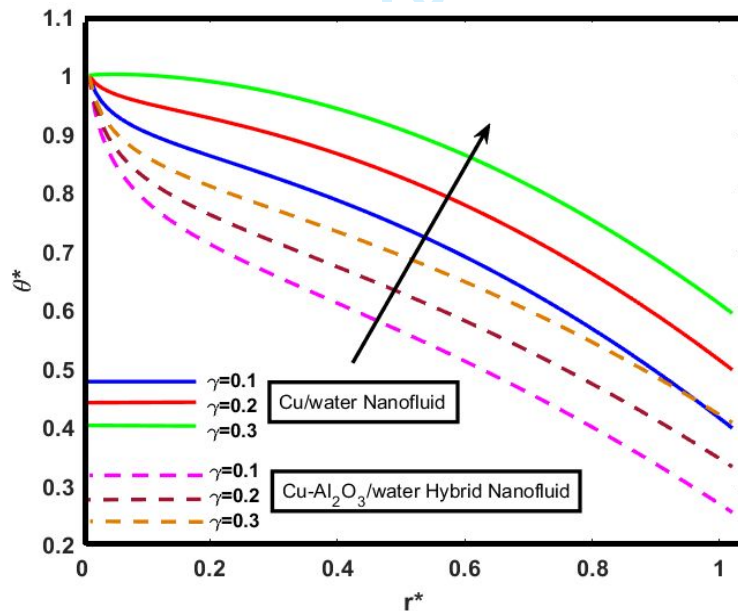$$\varphi_1 = 0.1, \varphi_2 = 0.0 \ (Cu/water \ Nanofluid).$$
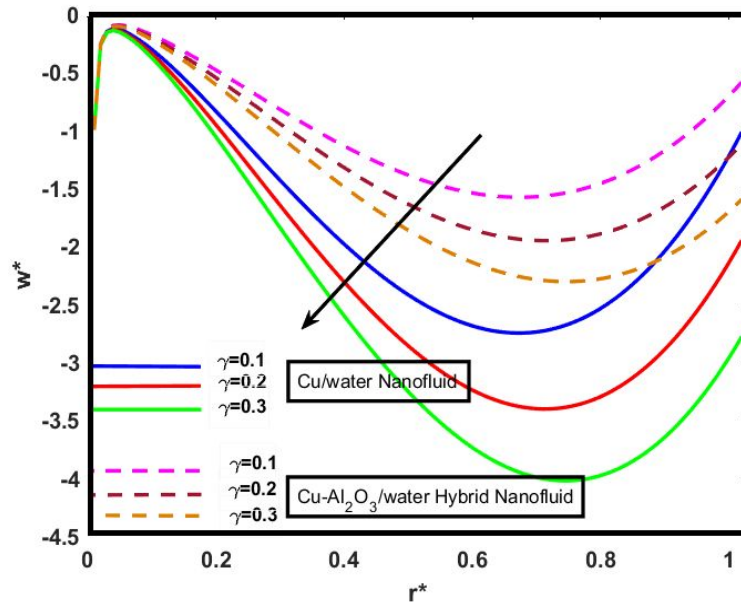
Fig. 4: Velocity distribution for different values of γ and $L = 0.1$, $z^* = 0.2$, $\lambda = 0.1$, $G_r^* = 0.2$, M=2,

$Q = 0.01, t^{**} = 0.2, k^* = 0.1, m' = 3.7, B = 0.4,$

$\varphi_1 = 0.1, \varphi_2 = 0.02 \left(Cu - Al_2O_3/water\ Nanofluid\right),$

$\varphi_1 = 0.1, \varphi_2 = 0.0 \left(Cu/water\ Nanofluid\right).$
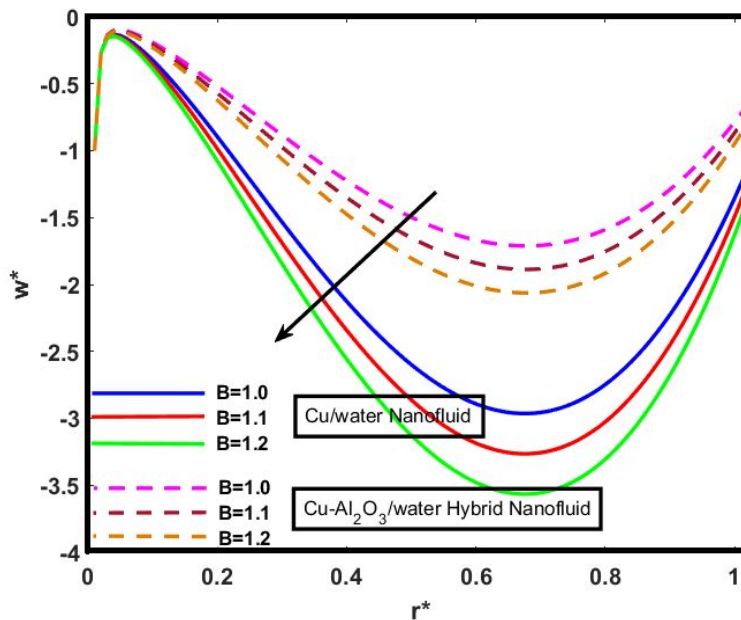
Fig. 5: Velocity distribution for different values of B and $L = 0.1$, $z^* = 0.2$, $\lambda = 0.1$, $G_r^* = 0.2$,

M=2, $Q = 0.01, t^{**} = 0.2, k^* = 0.1, m' = 3.7, \gamma = 0.1,$

$\varphi_1 = 0.1, \varphi_2 = 0.02 \left(Cu - Al_2O_3/water\ Nanofluid\right),$

17

$$\varphi_1 = 0.1, \varphi_2 = 0.0 \ (Cu/water\ Nanofluid).$$
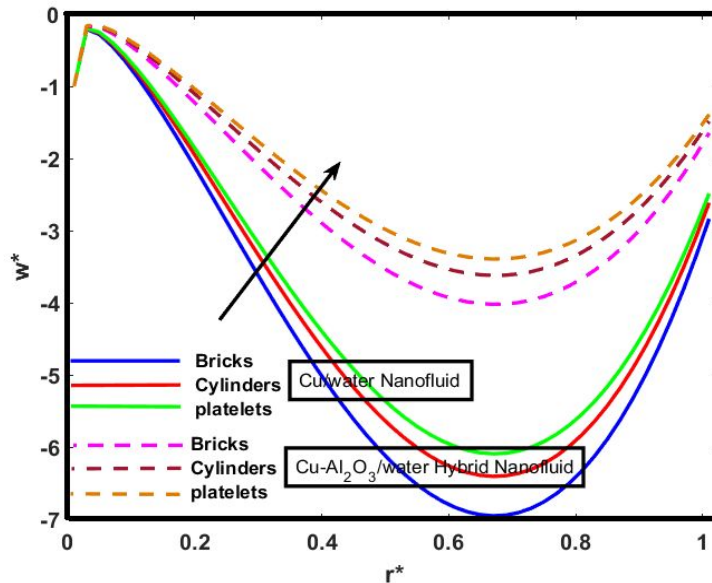
Fig. 6: Velocity distribution for different shapes (m') and $L = 0.1$, $z^* = 0.2$, $\lambda=0.1$, $G_r^* =0.2$, M=2, $Q = 0.01$, $t^{**} = 0.2$, $k^* = 0.1$, $B = 1.0$, $\gamma = 0.1$, $$\varphi_1 = 0.1, \varphi_2 = 0.02 \ (Cu - Al_2O_3/water\ Nanofluid),$$ $$\varphi_1 = 0.1, \varphi_2 = 0.0 \ (Cu/water\ Nanofluid).$$

Figs. (7-8) show the influence of heat absorption and slip effects on temperature profile. It is clearly observed that increasing values of heat absorption significantly increases temperature and shows elevation for hybrid nanofluid. Fig. 8 depicts that temperature profile has increasing behavior for large values of slip parameter and it shows that Cu-water nanofluid causes high temperature as compared to hybrid nanofluid.

18
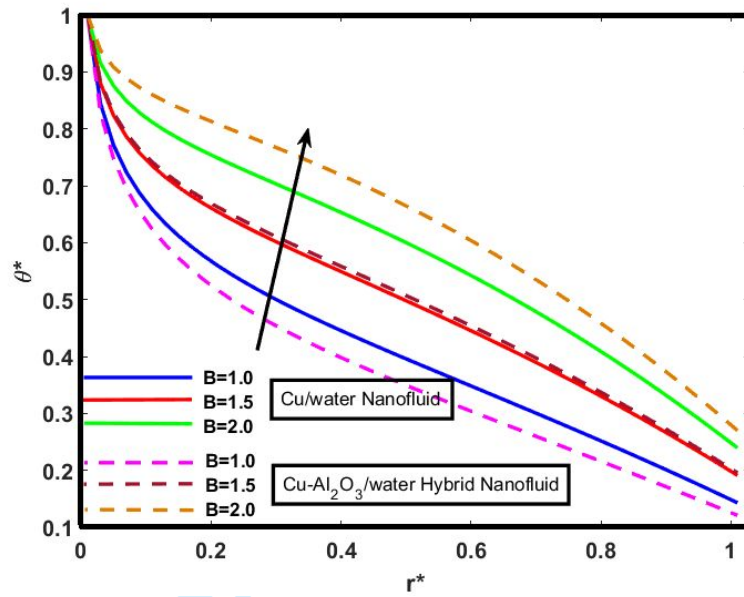
Fig. 7: Temperature distribution for different values of B and $z^* = 0.2$, $\lambda = 0.2$, $G_r^* = 0.2$, $M = 2$,

$$Q = 0.01, t^{**} = 0.2, k^* = 1.2, = 1.0, \gamma = 0.2,$$

$$\varphi_1 = 0.1, \varphi_2 = 0.06 \ (Cu - Al_2O_3/water \ Nanofluid),$$

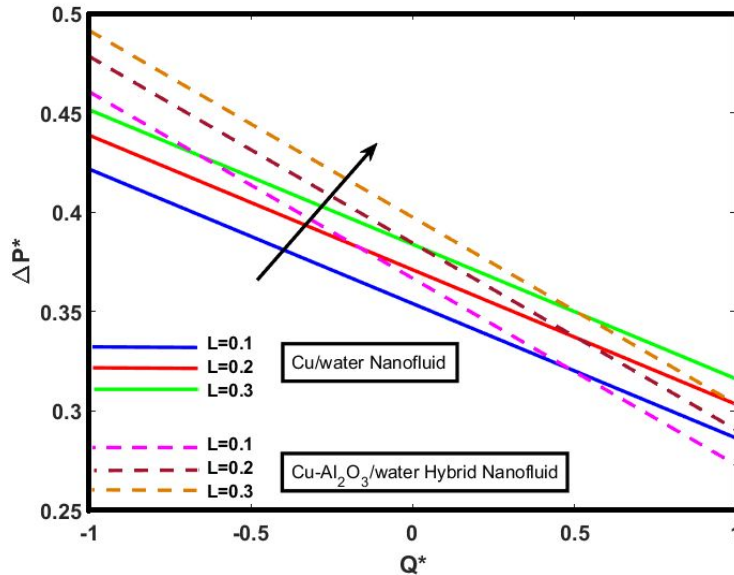$$\varphi_1 = 0.1, \varphi_2 = 0.0 \ (Cu/water \ Nanofluid).$$

Fig. 8: Temperature distribution for different values of γ and $z^* = 0.2$, $\lambda = 0.2$, $G_r^* = 0.2$, $M = 2$,

$$Q = 0.01, t^{**} = 0.2, k^* = 1.2, = 1.0, B = 2.0,$$

$$\varphi_1 = 0.1, \varphi_2 = 0.06 \ (Cu - Al_2O_3/water \ Nanofluid),$$

$$\varphi_1 = 0.1, \varphi_2 = 0.0 \ (Cu/water \ Nanofluid).$$

19

Pressure rise per wavelength is related to the effects of parameters in three different regions. The behavior is drawn in Figs. (9-12). Fig. 9 depicts that pressure rise per wavelength augments (Cu-water) nanofluid as compared to hybrid nanofluid. It is observed that buoyancy forces are more dominant in retrograde and reciprocal in peristaltic pumping region. Effects of velocity slip parameter are portrayed in Fig. 10. It is observed that higher velocity slip shows increasing behavior on pressure rise per wavelength. Same behavior of pressure rise per wavelength is witnessed Fig. 11 for thermal slip parameter. Hybrid nanofluid shows higher effects rather than Copper water nanofluid. Fig. 12 depicts different nanoparticle shape effects and plot shows that platelets shape nanoparticles show increasing behavior as compared to cylinder and bricks shape nanoparticles. It is also analyzed that hybrid nanofluid shows maximum influence than Cu-water nanofluid.
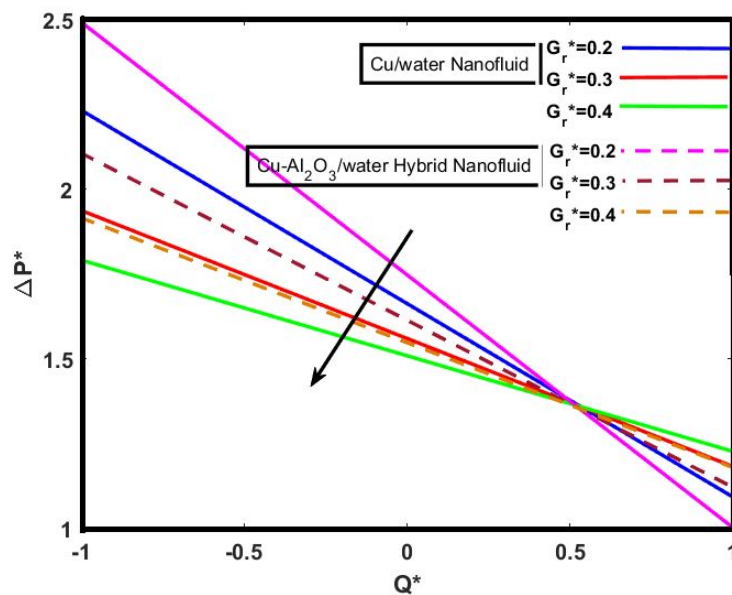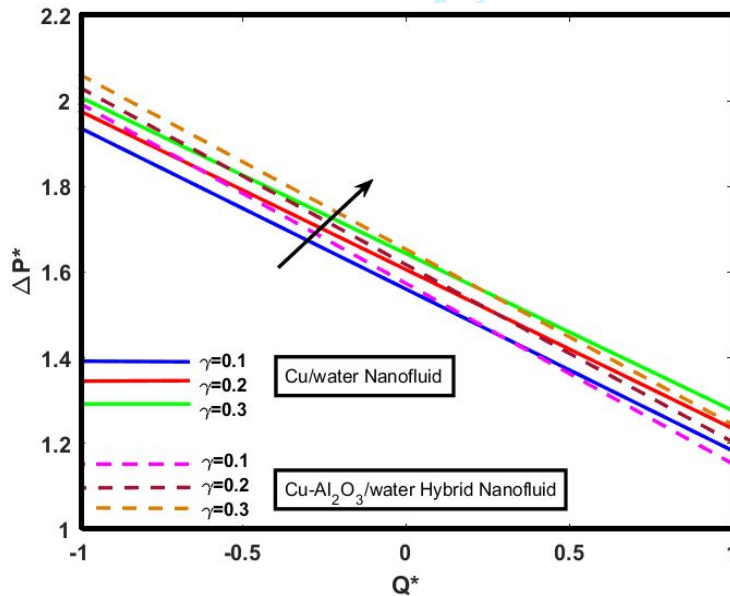

Fig. 9: Pressure rise for different values of G_r and $L = 0.1$, $z^* = 0.2$, $\lambda = 0.01$, $M = 1.5$, $Q = 0.01$,

$$t^{**} = 0.1, k^* = 0.3, B = 0.2, \gamma = 0.2, m' = 3.7,$$

$$\varphi_1 = 0.1, \varphi_2 = 0.04 \left(Cu - Al_2O_3/water\ Nanofluid \right),$$

$\varphi_1 = 0.1, \varphi_2 = 0.0 \; (Cu/water \; Nanofluid).$

Fig. 10: Pressure rise for different values of L and $z^* = 0.2$, $\lambda = 0.01$, M=1.5, $Q = 0.01$, $t^{**} = 0.1$,

$k^* = 0.3, B = 0.2, \gamma = 0.2, G_r^* = 0.4, m' = 3.7,$

$\varphi_1 = 0.1, \varphi_2 = 0.05 (Cu - Al_2O_3/water \; Nanofluid),$

$\varphi_1 = 0.1, \varphi_2 = 0.0 \; (Cu/water \; Nanofluid).$

Fig. 11: Pressure rise for different values of γ and $L = 0.1$, $z^* = 0.2$, $\lambda = 0.01$, M=1.5, $Q = 0.01$,

$t^{**} = 0.1, k^* = 0.3, B = 0.2, \gamma = 0.2, G_r^* = 0.4, m' = 3.7$

$\varphi_1 = 0.1, \varphi_2 = 0.05 (Cu - Al_2O_3/water \; Nanofluid),$

21

$$\varphi_1 = 0.1, \varphi_2 = 0.0 \; (Cu/water \; Nanofluid).$$
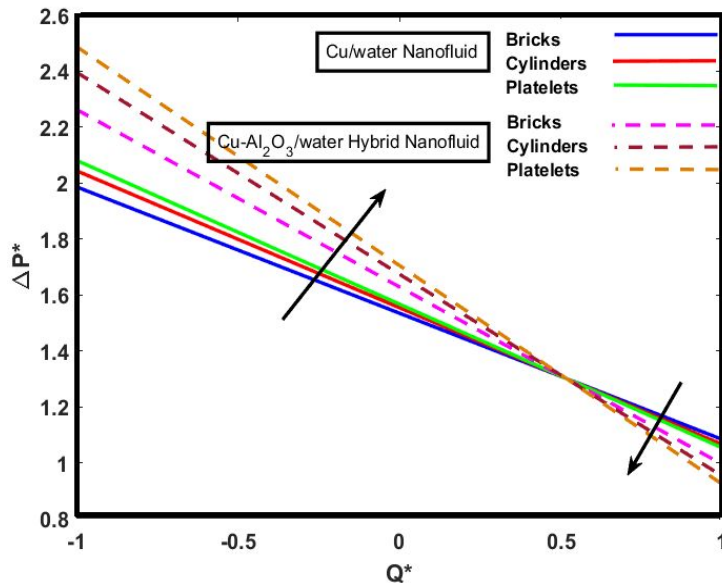
Fig. 12: Pressure rise for different shapes (m) and $L = 0.1$, $z^* = 0.2$, $\lambda = 0.01$, $M = 1.7$, $Q = 0.01$, $t^{**} = 0.1$, $k^* = 0.3$, $B = 0.2$, $\gamma = 0.2$, $G_r^* = 0.2$,

$$\varphi_1 = 0.1, \varphi_2 = 0.05 (Cu - Al_2O_3/water \; Nanofluid),$$

$$\varphi_1 = 0.1, \varphi_2 = 0.0 \; (Cu/water \; Nanofluid).$$

Figs. (13-17) demonstrate the consequences of variations of slip parameters, Magnetic field, heat absorption parameter and different shape effects. Impacts of slip parameters plotted in Figs. (13-17). Fig. 13 shows that longitudinal pressure gradient is maximum for larger values of velocity slip parameter and it also depicts that copper water nanofluid has higher increase as compare to hybrid nanofluid. Fig. 14 illustrates that higher values of thermal slip parameter yields enhancement in pressure gradient and hybrid nanofluid has higher impact than cu-water nanofluid. It is observed from Fig. 15 that the pressure gradient increases for larger values of magnetic field. Meanwhile, electromagnetic forces are useful for increasing pressure gradient and it goes higher for Cu-water nanofluid near the upper wall. Fig. 16 portrays the effects of heat absorption parameter and shows that pressure gradient decreases by increasing heat absorption parameter and Cu-water nanofluid has larger impact as compare to hybrid nanofluid. Different nanoparticle shape

effects are displayed in Fig. 17 and it represents that platelets shape nanoparticles of hybrid nanofluid has more significant effect on pressure gradient as compare to cylinder and bricks shape nanoparticles of Cu-water nanofluid. Finally, the heat transfer phenomenon is discussed in Fig. 18 and confirms that Cu-water nanofluid has larger impact for increasing values of heat absorption than hybrid nanofluid.
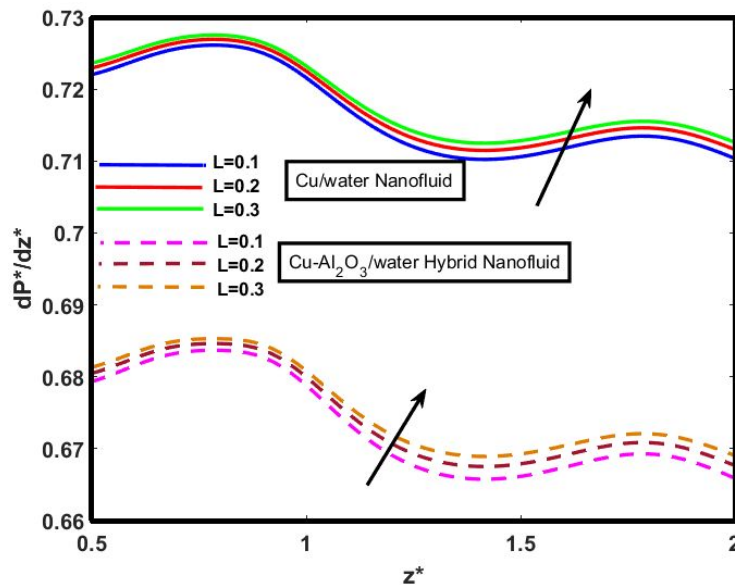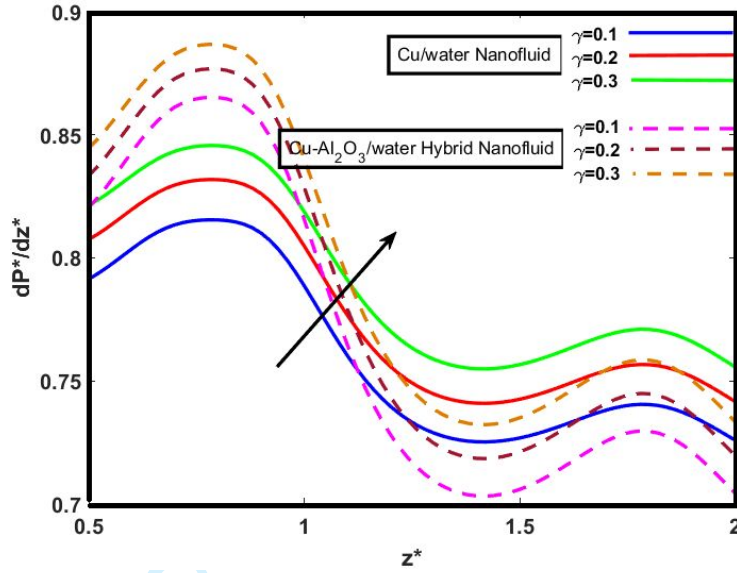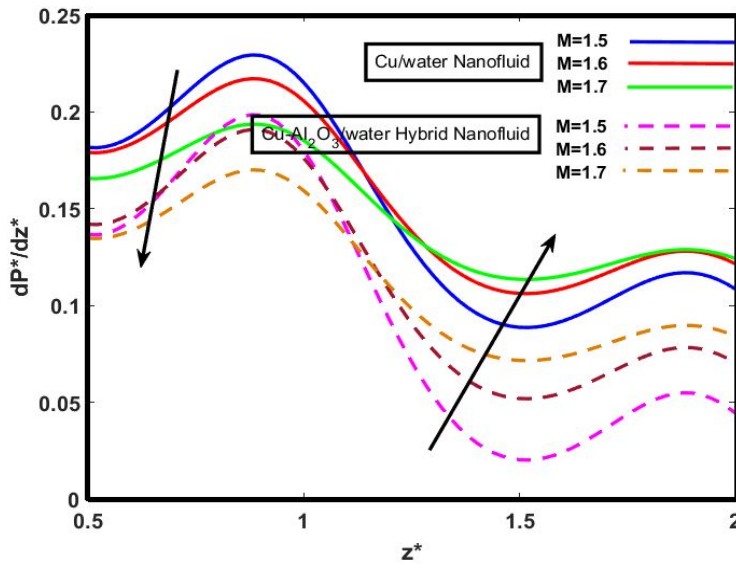

Fig. 13: Pressure gradient for different values of L and $z^* = 0.2$, $\lambda = 0.01$, M=1.5, $t^{**} = 0.1$, k^* = 1.2, $B = 0.2$, $\gamma = 0.2$, $G_r^* = 0.4$, $m' = 3.7$,

$$\varphi_1 = 0.1, \varphi_2 = 0.05 (Cu - Al_2O_3/water\ Nanofluid),$$
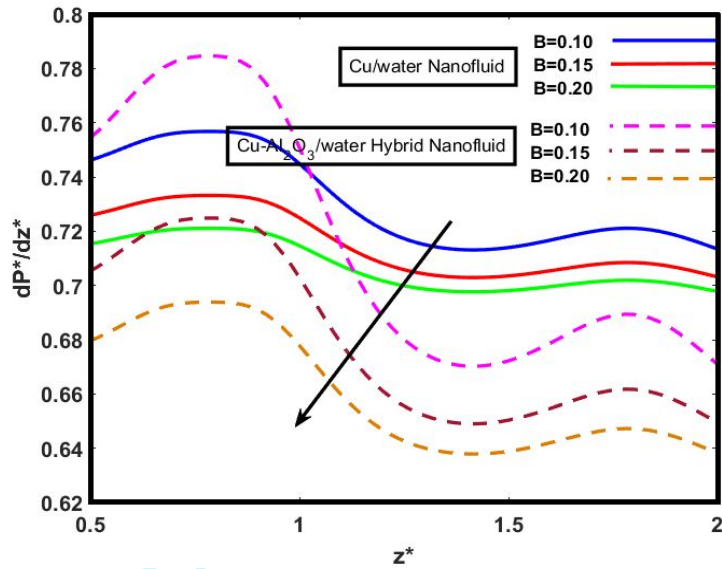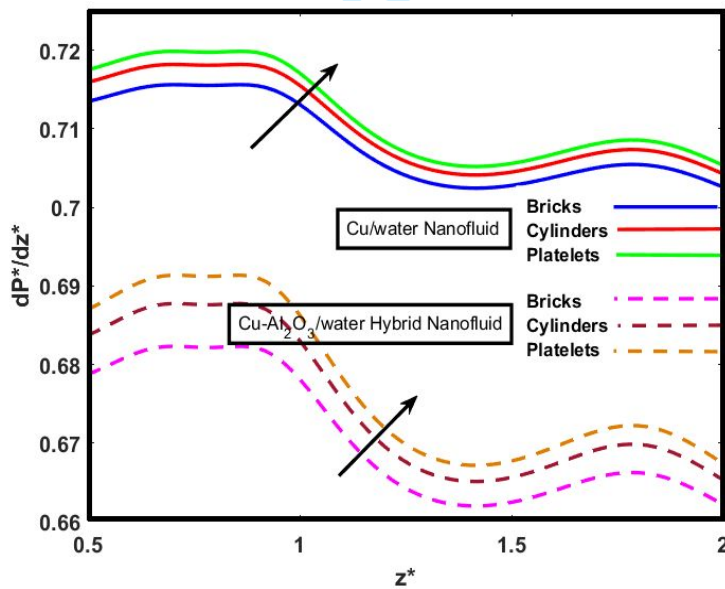
$$\varphi_1 = 0.1, \varphi_2 = 0.0\ (Cu/water\ Nanofluid).$$

Fig. 14: Pressure gradient for different values of γ and $L = 0.1$, $z^* = 0.2$, $\lambda=0.01$, M=2.0, t^{**}
$= 0.1$, $k^* = 1.2$, $B = 0.2$, $\gamma = 0.2$, $G_r^* = 0.1$, $m'=3.7$,

$$\varphi_1 = 0.1, \varphi_2 = 0.02 \big(Cu - Al_2O_3/water \ Nanofluid\big),$$

$$\varphi_1 = 0.1, \varphi_2 = 0.0 \ \big(Cu/water \ Nanofluid\big).$$

Fig. 15: Pressure gradient for different values of M and $L = 0.1$, $z^* = 0.2$, $\lambda=0.01$, $t^{**} = 0.1$, k^*
$= 1.2$, $B = 0.2$, $\gamma = 0.2$, $G_r^* = 0.2$, $m'=3.7$,

$$\varphi_1 = 0.1, \varphi_2 = 0.05 \big(Cu - Al_2O_3/water \ Nanofluid\big),$$

$$\varphi_1 = 0.1, \varphi_2 = 0.0 \ \big(Cu/water \ Nanofluid\big).$$

24

Fig. 16: Pressure gradient for different values of B and $L = 0.1$, $z^* = 0.2$, $\lambda = 0.01$, M=2.0, t^{**}

$$= 0.1, k^* = 1.2, \gamma = 0.1, \gamma = 0.2, G_r^* = 0.2, m' = 3.7,$$

$$\varphi_1 = 0.1, \varphi_2 = 0.04 (Cu - Al_2O_3/water\ Nanofluid),$$
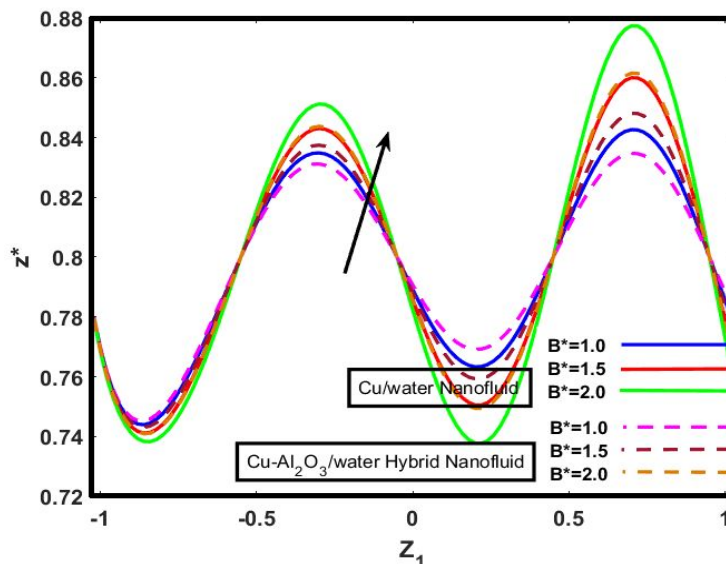
$$\varphi_1 = 0.1, \varphi_2 = 0.0\ (Cu/water\ Nanofluid).$$

Fig. 17: Pressure gradient for different shapes (m') and $L = 0.1$, $z^* = 0.2$, $\lambda = 0.01$, M=2.0, t^{**}

$$= 0.1, k^* = 1.2, \gamma = 0.1, \gamma = 0.2, G_r^* = 0.2, B = 0.1,$$

$$\varphi_1 = 0.1, \varphi_2 = 0.02 (Cu - Al_2O_3/water\ Nanofluid),$$

$$\varphi_1 = 0.1, \varphi_2 = 0.0\ (Cu/water\ Nanofluid).$$

Fig. 18: Heat transfer for different values of B and $z^* = 0.2$, $\lambda = 0.2$, $t^{**} = 0.2$, $k^* = 1.2$, $\gamma = 0.1$,

$$\gamma = 0.2, m' = 3.7,$$

$$\varphi_1 = 0.1, \varphi_2 = 0.06 \left(Cu - Al_2O_3/water\ Nanofluid \right),$$

$$\varphi_1 = 0.1, \varphi_2 = 0.0 \left(Cu/water\ Nanofluid \right).$$

Trapping

Trapping signifies an attention-grabbing phenomenon for the flow of fluid in a divergent tube. Contour, under certain conditions, describe to trap a bolus that moves as a whole with the average speed on the section of the tube. The formation of an internal bolus of the fluid by a stream line is always closed. The bolus is defined as a volume of the fluid delimited by a closed contour in a tube.

Figs. (19-22) are plotted to show the flow Pattern of Cu-water and (Cu- Al_2O_3)/ water in a tube for thermal slip parameter. It can be observed that more bolus appears for Cu-water nanofluid as compare to (Cu- Al_2O_3)/water. Figs. (23-26) describes the impact of non-uniform parameter for Cu-water and (Cu- Al_2O_3)/water in a tube. It is evident that the quantity of the bolus increases for large values of non-uniform parameter and shows the same behavior for Cu-water and (Cu-Al_2O_3)/water fluid. It is also extracted in Figs. Figs. (27-30) that the size of the bolus enlarges for

26

large value velocity slip parameter and has same behavior for Cu-water and hybrid nanofluid. Figs. (31-33) describes the influence of nanoparticle shape parameter on the trapping pattern. These panels show that the number of the bolus reduces for bricks and cylinder shapes particles, however, the size of the trapped bolus enlarges for platelets shapes of nanoparticles.
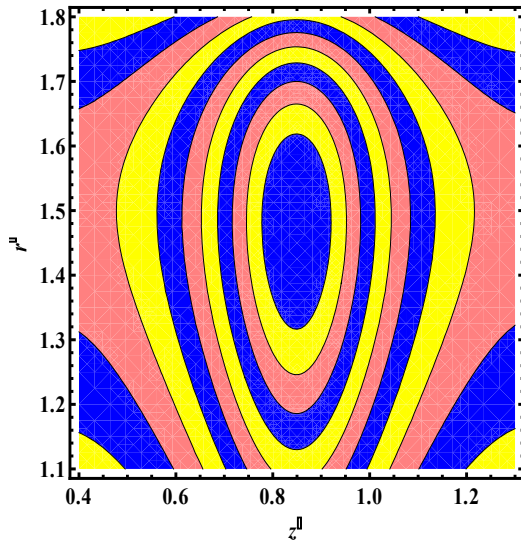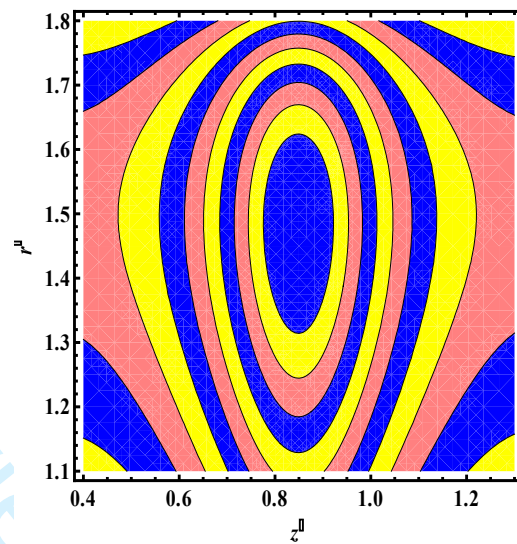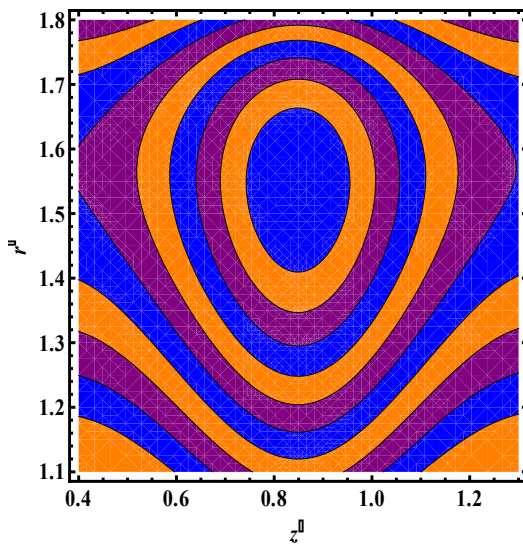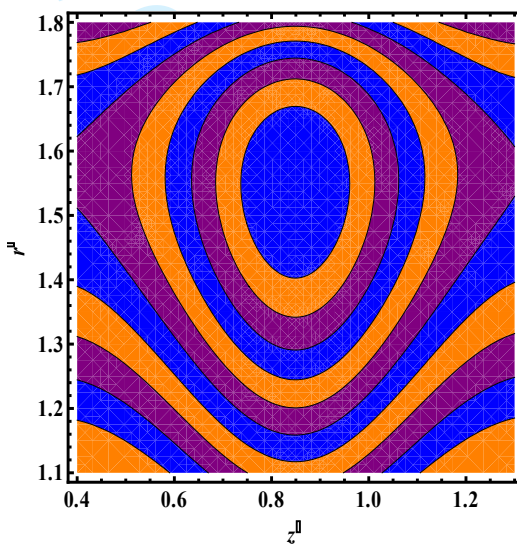

Fig. 19

Fig. 20

Fig. 21

Fig. 22

Figs. (19-20) Configuration of Cu-water through a tube for

(i) γ(thermal slip paramaten) $= 2,4$ (ii) $\varphi_1 = 0.1, \varphi_2 = 0.0$

27

(21-22) Configuration of Cu- Al_2O_3/water through a tube for

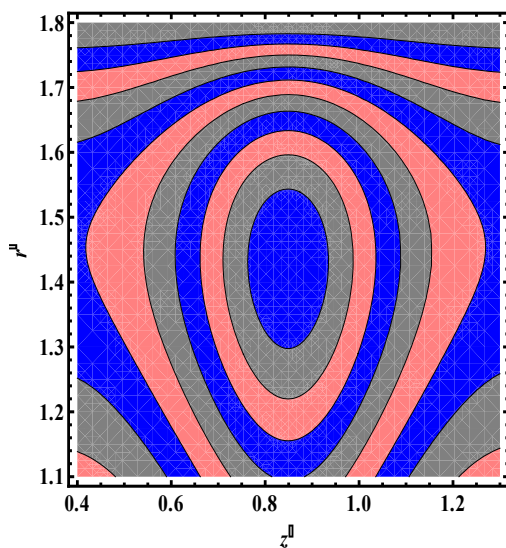(i) γ(thermal slip parameter) = 2,4 (ii) $\varphi_1 = 0.1$, $\varphi_2 = 0.05$

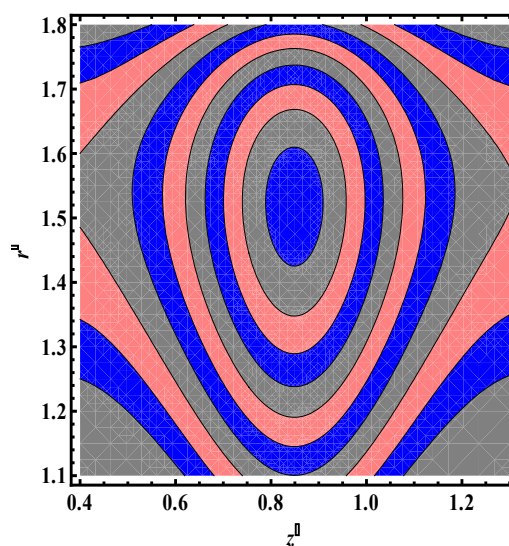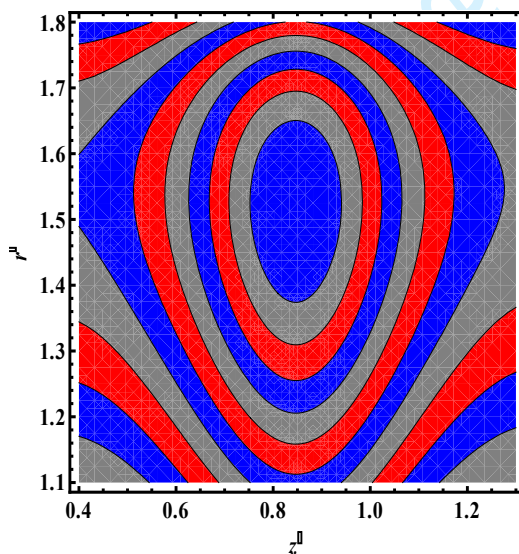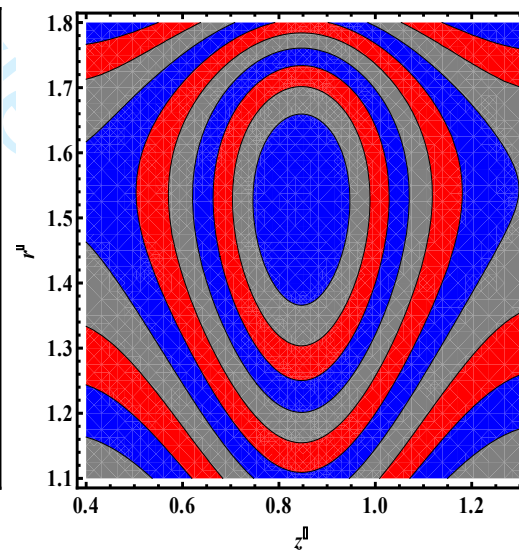**Fig. 23**

Fig. 24

Fig. 25

Fig. 26

Figs. (23-24), Configuration of Cu-water through a tube for

(i) k^* (non-uniform parameter) = 0.01, 0.03   (ii) $\varphi_1 = 0.1$, $\varphi_2 = 0.0$

Figs. (25-26), Configuration of Cu- Al_2O_3/water through a tube for

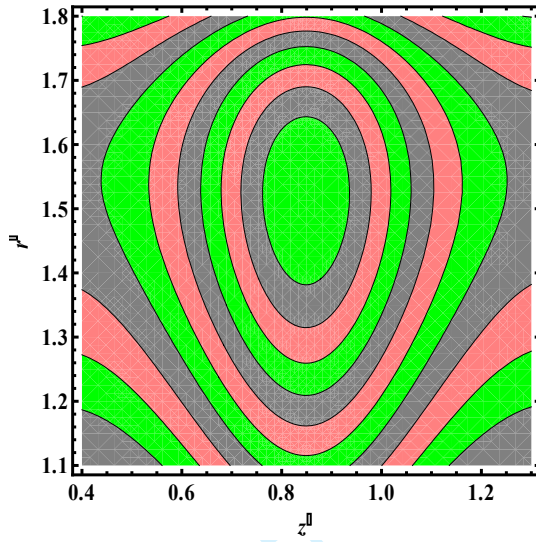(i) k^* (non-uniform parameter) = 0.01, 0.03   (ii) $\varphi_1 = 0.1$, $\varphi_2 = 0.06$
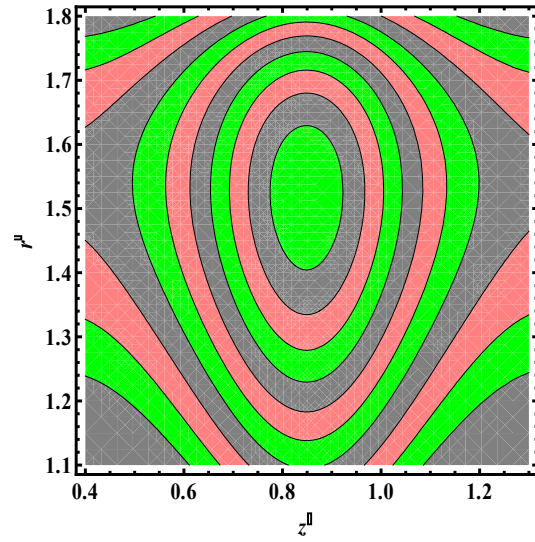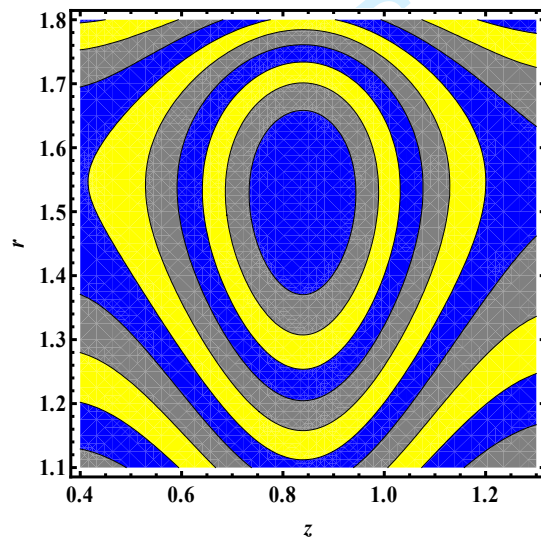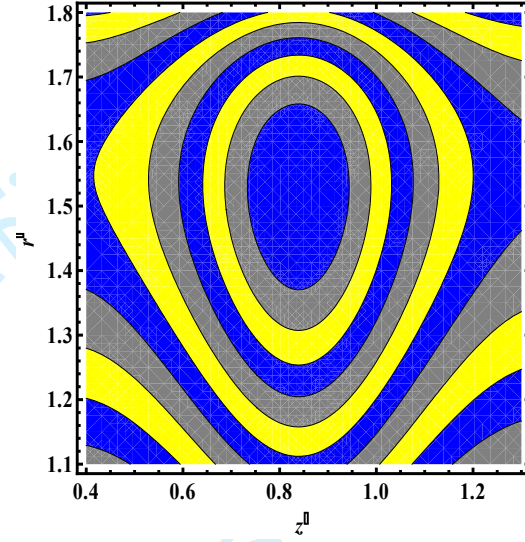
28

Fig. 27

Fig. 28

Fig. 29

Fig. 30

Figs. (27-28), Configuration of Cu-water through a tube for

(i) L (Velocity slip parameter) = 1.2, 1.4 (ii) $\varphi_1 = 0.1, \varphi_2 = 0.0$

Figs. (29-30), Configuration of Cu- Al_2O_3/water through a tube for

(i)L (Velocity slip parameter) = 1.2, 1.4 (ii) $\varphi_1 = 0.1, \varphi_2 = 0.04$
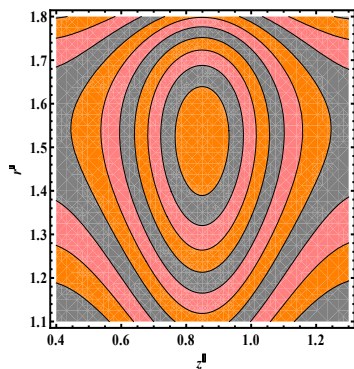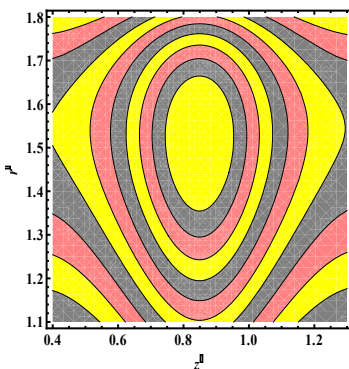
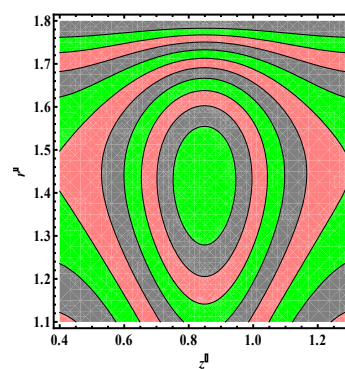**Fig. 31**   **Fig. 32**   **Fig. 33**

Figs. (31-33), Configuration of Cu- Al_2O_3/water through a tube for Different shape effects (i) Bricks (ii) cylinder (iii) Platelets (iv) $\varphi_1 = 0.1, \varphi_2 = 0.05$

5. Conclusions

Aforementioned research focusses on the nanoparticles shape, slip effects and heat transfer on steady physiological delivery of MHD hybrid nanofluid with peristaltic motion in a tube. Limited study is carried out on the research regarding phenomenon for hybrid nanofluids till now. The exact solutions of the emerging problem are obtained by plotting graphs against theoretical study. The relevant results can be concluded as

- Velocity profile reveals that Cu-water/nanofluid is slower than the hybrid nanofluid for large values of slip parameters.

- In a temperature distribution, heat absorption parameter are more substantial as fluid flow speeds up when large values are chosen.

- Effects of Grashof number pictured that pressure rise per wavelength enhances for cu-water nanofluid as compared to hybrid nanofluid. Results also show that buoyancy forces are more dominant in retrograde and elevated peristaltic pumping region.

30

- Effects of shape of the different nanoparticle on pressure rise per wavelength shows that bricks shape nanoparticles have more decreasing behavior as compared to cylinder and platelets shape nanoparticles.

- Large values of thermal slip parameter enhance pressure gradient and cu-water nanofluid has higher impact than hybrid nanofluid.

- Platelets shape nanoparticles of hybrid nanofluid has more significant effect on pressure gradient as compare to cylinder and bricks shape nanoparticles of Cu-water nanofluid.

- The size of trapped bolus enlarges for bricks shapes nanoparticles while decreases for platelets and cylinder shapes nanoparticles.

31

References

[1] W. M. Bayliss, E. H. Starling, The movement and innervation of the small intestine, The Journal of Physiology. 24(1899)99–143.

[2] T. W. Latham, Fluid motion in a peristaltic pump [M.S. thesis], Massachusetts Institute of Technology, Cambridge, Mass. USA (1966).

[3] M. Y. Jaffrin, A. H. Shapiro, Peristaltic pumping, Annual Review of Fluid Mechanics. 3(1971)13–36.

[4] Y. V. K. R. Kumar, P. S. V. H. N. K. Kumari, M. V. R. Murthy, and S. Sreenadh, Unsteady peristaltic pumping in a finite length tube with permeable wall, Journal of Fluids Engineering. 132(2010) Article ID.

[5] U.S. Choi, Enhancing thermal conductivity of fluids with nanoparticles, in: D.A. Siginer, H.P. Wang (Eds.), Developments and Applications of Non-Newtonian Flows FED. 66(1955)99–105.

[6] C.J. Ho a , J.B. Huang a , P.S. Tsai b , Y.M. Yang c, On laminar convective cooling performance of hybrid water-based suspensions of Al2O3 nanoparticles and MEPCM particles in a circular tube International Journal of Heat and Mass Transfer 54 (2011) 2397–2407.

[7] Z.H. Han, B. Yang, S.H. Kim, M.R. Zachariah, Application of hybrid sphere/carbon nanotube particles in nanofluids, Nanotechnology. 18(2007)105701.

[8] M.J. Nine, B. Munkhbayar, M.S. Rahman, H. Chung, H.Jeong, Highly productive synthesis process of well dispersed CuO_2 and $Cu=CuO_2$ nanoparticles and its thermal characterization, Mat. Chem. Phys. 141(2013)636–642.

[9] D. Toghraie, V.A. Chaharsoghi, M. Afrand, Measurement of thermal conductivity of ZnO _ $TiO_2=EG$ hybrid nanofluid: effects of temperature and nanoparticles concentration, J.Therm. Anal. Calorim (2016) 01654364.

[10] J. Sarkar, P. Ghosh, A. Adil, A review on hybrid nanofluids: recent research development and applications, Renew. Sustain. Energy Rev. 43(2015)164–177.

[11] W.S. Han, S.H. Rhi, Thermal characteristics of grooved heat pipe with hybrid nanofluids, Therm. Sci. 15 (2011) 195–206.

[12] P. Selvakumar, S. Suresh, Use of Al 2 O3–Cu / water hybrid nanofluid in an electronic heat sink, IEEE Trans Compon Packag Manuf. Technol. 2 (2012) 1600–1607.

[13] S. Suresh, K.P. Venkitaraj, P. Selvakumar, M. Chandrasekhar, Effect of Al_2O_3-Cu / water hybrid nanofluid in heat transfer, Exp. Therm. Fluid Sci. 38(2012) 54–60.

[14] R. Nimmagadda, K. Venkatasubbaiah, Conjugate heat transfer analysis of micro channel using novel hybrid nanofluids (Al2 O3 + Ag/Water), Eur. J. Mech. B Fluids 52 (2015) 19–27.

[15] H.R. Allahyar, F. Hormozi, N. B. Zare, Experimental investigation on the thermal performance of a coiled heat exchanger using a new hybrid nanofluid, Exp. Therm. Fluid Sci. 76 (2016) 324-329.

[16] D. Huang, Z. Wu, B. Sunden, Effects of hybrid nanofluid mixture in plate heat exchangers, Exp. Therm. Fluid Sci. 72(2016)190-196.

[17] B. Takabi, A. M. Gheitaghy, P. Tazraei, Hybrid water-based suspension of Al2 O3 and Cu nanoparticles on laminar convection effectiveness, J. Thermophys. Heat Transf. 30(3) (2016) 523-532.

[18] S. S. U. Devi, S.P. A. Devi, Numerical investigation of three-dimensional hybrid CuAl2 O3/water nanofluid flow over a stretching sheet with effecting Lorentz force subject to Newtonian heating, Can. J. Phys. 94(5) (2016) 490-496.

[19] A. Ahammed, L.G. Asirvatham, S. Wongwises, Entropy generation analysis of graphene alumina hybrid nanofluid in multiport minichannel heat exchanger coupled with thermoelectric cooler, Int. J. Heat Mass Transf. 103 (2016) 1084-1097.

[20] L. C. Woods, Thermodynamics of Fluid Systems, Oxford University Press, Oxford, UK, 1975.

[21] D. Cimpean, N. Lungu, I. Pop, A problem of entropy generation in a channel filled with a porous medium, Creative Math. Inf. 17(2008) 357-362.

[22] H. F. Öztop, E. Abu-Nada, Numerical study of natural convection in partially heated rectangular enclosures filled with nanofluids, Int. J. Heat and Fluid Flow. 29(2008)13261336.

[23] O. D. Makinde, Z. H. Khan, W. A. Khan, M. S. T. Shehla, Magneto hemodynamics of nanofuid with heat and mass transfer in a slowly varying symmetrical channel, International Journal of Engineering Research in Africa. 28(2017) 118-141.

[24] M. M. Bhatti, R. Ellahi, A. Zeeshan, Study of variable magnetic field on the peristaltic flow of Jeffery fluid in a non-uniform rectangular duct having compliant walls, Journal of Molecular Liquids. 222(2016) 101-108.

[25] A. T. Olatundun, O. D. Makinde, Analysis of Blasius flow of hybrid nanofluids over a convectively heated surface, Defect and Discusion Forum. 377(2017) 29-41.

[26] M. M. Bhatti, M. Sheikholeslami, A. Zeeshan, Entropy analysis on electro-kinetically modulated peristaltic propulsion of magnetized nanofluid flow through a microchannel, Entropy. 19(2017) 481.

[27] S. U. S. Choi, Enhancing thermal conductivity of fluids with nanoparticles, In: Siginer DA, Wang HP (Eds), Developments and applications of non-Newtonian flows, ASME, 36(1995) 99-105.

[28] R. Ellahi, M. M. Bhatti, C. M. Khalique, Three-dimensional flow analysis of Carreau fluid model induced by peristaltic wave in the presence of magnetic field, Journal of Molecular Liquids. 241(2017) 1059-1068.

[29] M. G. Reddy, O. D. Makinde, Magneto hydrodynamic peristaltic transport of Jeffery nanofluid in an asymmetric channel, Journal of Molecular Liquids. 223(2016)1242-1248.

[30] M. M. Bhatti, A. Zeeshan, R. Ellahi, N. Ijaz, Heat and mass transfer of two-phase flow with Electric double layer effects induced due to peristaltic propulsion in the presence of transverse magnetic field, Journal of Molecular Liquids. 230(2017) 237-246.

[31] M. G. Reddy, K. Venugopal Reddy, O. D. Makinde, Hydromagnetic peristaltic motion of a reacting and radiating couple stress fluid in an inclined asymmetric channel with a porous medium, Alexandria Engineering Journal, 55(2016) 1841-1853.

[32] M. M. Bhatti, M. M. Rashidi, Effects of thermo-discussion and thermal radiation on Williamson nanofluid over a porous shrinking/stretching sheet, Journal of Molecular Liquids. 221(2016) 567-573.

[33] B. C. Sarkar, S. Das, R. N. Jana, O. D. Makinde, Magneto hydrodynamic peristaltic flow of nanofluids in a convectively heated vertical asymmetric channel in presence of thermal radiation, Journal of Nanofluids. 4(2015) 461-473.

[34] M. M. Bhatti, M. A. Abbas, M. M. Rashidi, A robust numerical method for solving stagnation point flow over a permeable shrinking sheet under the influence of MHD, Applied Mathematics and Computation, 316(2017) 381-389.

[35] I. Khan, Z. Li, A. Shaffee, I.Tilli, T. Asifa, Energy transfer of Jeffery–Hamel nanofluid flow between non-parallel walls using Maxwell–Garnetts (MG) and Brinkman models. Energy Reports, (4) 2018, 393-399.

[36] MI. Afridi, M. Qasim, I. Khan, I. Tilli, Entropy generation in MHD mixed convection stagnation-point flow in the presence of joule and frictional heating. Case studies in Thermal Engineering, 12 (2018), 292-300

[37] A. Khalid, I. Khan, A. Khan, S. Shafie, I. Tilli, Case study of MHD blood flow in a porous medium with CNTS and thermal analysis, Case Studies in Thermal Engineering, 12 (2018), 374-380

[38] I. Khan, KA. Abro, MN. Mirbhar, I. Tilli, Thermal analysis in stokes' second problem of nanofluid: Applications in thermal engineering, Case Studies in Thermal Engineering, 12 (2018), 271-275.

[39] KA. Abro, MM. Rashidi, I. Khan, IA. Abro, A. Tassaddiq, Analysis of stokes' Second problem for Nanofluids Using Modern Approach of Atangana- Baleanu Fractional Derivative, Journal of Nanofluids, 7 (2018), 738-747.

[40] S. Aman, I. Khan, Z. Ismail, MZ. Salleh, Impacts of gold nanoparticles on MHD mixed convection Poiseuille flow of nanofluid passing through a porous medium in the presence of thermal radiation, thermal diffusion and, Neural Computing and Applications, 30 (2018), 789-797.

[41] A. Khan, D. Khan, I. Khan, F. Ali, F ul Karim, M. Imran, MHD flow of sodium Alginate-Based Casson Type Nanofluid Passing Through A Porous Medium With Newtonian Heating, Scientific Reports, 8(2018), 8645.

[42] S. Aman, I. Khan, Z. Ismail, MZ. Salleh, I. Tlili, A new Caputo fractional model for heat transfer enhancement of water basedgraphene nanofluid: An application to solar energy, Results in physics, 9 (2018), 1352-1362.

[43] A. Gul, I. Khan, SS. Makhanov, Entropy generation in a mixed convection Poiseulle flow of molybdenum disulphide Jeffery nanofluid, Results in Physics, 9 (2018), 947-954.

[44] A. Hussanan, MZSalleh, I. Khan, Microstructure and inertial characteristics of a magnetite ferrofluid over a stretching/ shrinking sheet using effective thermal conductivity model, Journal of Molecular Liquids, 255(2018), 64-75.

[45] TN. Ahmed, I. Khan, Mixed convection flow of sodium alginate (SA-NaAlg) based molybdenum disulphide (MoS2) nanofluids: Maxwell Garnetts and Brinkman models, Results in Physics, 8 (2018), 752-757.

[46] I. Tlili, WA. Khan, I. Khan, Multiple slips effects on MHD SA-Al_2O_3 and SA-Cu non-Newtonian nanofluids flow over a stretching cylinder in porous medium with radiation and chemical reaction, Results in Physics, 8 (2018), 213-222.

[47] M. Saqib, F. Ali, I. Khan, NA. Sheikh, A. Khan, Entropy generation in Different Types of Fractionalized Nanofluids, Arabian Journal for Science and Engineering, (2018), 1-10.

[48] N. Iftikhar, A. Rehman, H. Sadaf and M. Khan, Impact of wall properties on the peristaltic flow of Cu-water nano fluid in a non-uniform inclined tube. International Journal of Heat and Mass Transfer, 125 (2018), 772-779.

[49] N. Iftikhar, A. Rehman, Peristaltic flow of an Eyring Prandtl fluid in a diverging tube with heat and mass transfer, International Journal of Heat and Mass Transfer, 111 (2017), 667-676.

[50] N. Iftikhar, A. Rehman and M. Khan, Features of convective heat transfer on MHD peristaltic movement of Williamson fluid with the presence of Joule heating, IOP Conference Series: Materials Science and Engineering, 414 (2018) 012010 doi: 10.1088/1757-899X/414/012010.

[51] Z. Iqbal, N. S. Akbar, E. Azhar, Performance of hybrid nanofluid (Cu-CuO/water) on MHD rotating transport in oscillating vertical channel inspired by Hall current and thermal radiation, Alexandria Eng. J. (2017), article in Press.